

Magnetic Resonance Imaging in 18 Horses with Palmar Foot Pain

Sue J. Dyson, VetMB, PhD; Rachel C. Murray, VetMB, PhD;
Michael C. Schramme, DVM, PhD; and Marion V. Branch, BSc

Magnetic resonance imaging can demonstrate core lesions, dorsal tears, and sagittal splits in the deep digital flexor tendon within the hoof capsule in horses with unilateral or bilateral palmar foot pain. Abnormalities of the navicular bone can be seen in horses with no detectable radiological abnormality. Lesions of the articular cartilage and subchondral bone of the distal interphalangeal joint can be identified. Authors' address: Centre for Equine Studies, Animal Health Trust, Lanwades Park, Kentford, Newmarket, Suffolk CB8 7UU, United Kingdom. © 2002 AAEP.

1. Introduction

Palmar foot pain is a common cause of equine lameness, but definitive diagnosis of the cause is often elusive. The specificity of local analgesic techniques has been questioned.¹⁻³ There is controversy about the interpretation of radiographs of the navicular bone, and it is clear that radiography is not a particularly sensitive indicator of navicular bone disease. Nuclear scintigraphy provides highly sensitive information about abnormal bone activity, but anatomical localization is limited and there is a relatively high incidence of false positive results.⁴ Ultrasonographic examination of the foot is limited to the sagittal midline, and off-incidence artifacts may confuse interpretation.^{5,6} Computed tomography (CT) can be used for accurate assessment of the three-dimensional (3D) distribution of both bone and soft tissue lesions, but this requires general anesthesia.⁷⁻¹⁰

There are a number of case reports describing lesions identified using magnetic resonance imaging (MRI) in horses with pain localized to the foot,¹¹⁻¹³

and a recent detailed study describing the use of imaging sequences to examine the osseous and soft tissue structures of the digit.¹⁴ Methodology for, and results of, MRI of the foot of live horses have recently been documented.^b

The purposes of this paper are to describe the results of MRI in horses with forelimb lameness in which pain was localized to the foot using perineural analgesia and in which there was improvement in lameness by either intra-articular analgesia of the distal interphalangeal (DIP) joint or intra-theal analgesia of the navicular bursa, and to correlate these with the results of other imaging modalities.

2. Materials and Methods

Eighteen horses with unilateral or bilateral forelimb lameness, with pain localized to the foot, were examined using MRI at the Animal Health Trust between January and December 2001. A definitive diagnosis of the cause of pain could not be established using radiography and ultrasonography.

All horses were subjected to a detailed clinical examination, with assessment of gait in straight

NOTES

RADIOLOGY

lines on a hard surface and in circles on the lunge of 10- to 15-m diameter on both soft and hard surfaces. Lameness was graded under each circumstance on a scale of 0–8 (0 = sound; 2 = mild; 4 = moderate; 6 = severe; 8 = non-weight bearing).

Local analgesic techniques employed included perineural analgesia of the palmar digital nerves and palmar (abaxial sesamoid) nerves (1.5–2 ml mepivacaine^g per site), intra-articular analgesia of the DIP joint (6 ml mepivacaine), and intra-theal analgesia of the navicular bursa (3–4 ml mepivacaine), performed under radiographic control. Lameness was reassessed 10 min after perineural analgesia and 5 min after intra-articular or intra-theal analgesia. Horses stood still after injection before re-evaluation of the gait in both straight lines and circles.

Radiographic examination was performed after removal of the shoes and appropriate preparation of the foot, using lateromedial, dorsoproximal-palmarodistal oblique, and palmarproximal-palmarodistal oblique views, and flexed oblique views of the interphalangeal joints and palmar processes of the distal phalanx.¹⁵

Ultrasonographic examination of the palmar soft tissues of the pastern was performed using a 10-MHz linear transducer, with and without a stand-off. A 6.5-MHz convex array transducer was used to examine the palmar aspect of the foot through the bulbs of the heel and through the center of the frog.

Nuclear scintigraphic examination of the feet was performed using vascular, pool, and bone phase images, and dorsal, lateral, and solar views were obtained with 2-min acquisition times.^{4,16} All horses were lunged for 15 min before injection of the radiopharmaceutical (1 GBq/100 kg of body weight).¹⁶

At least 2 wk elapsed between intra-synovial injections and MRI. Before MRI, all shoes were removed, and the feet to be examined were cleaned thoroughly. With the horse under general anesthesia, the forelimbs were positioned in the isocenter of a short-bore, flared-end 1.5-Tesla GE Signa Echo-speed magnet General Electric, Milwaukee. A human extremity radiofrequency (RF) coil was placed around the foot to be imaged. Sandbags were placed on the limbs to reduce movement associated with respiration.

A three-plane localizer image was obtained first to ensure correct positioning of the limbs and for orientation of subsequent sequences. Images were obtained in sagittal, transverse, and dorsal planes and included 3D T2^a gradient echo (GRE), spoiled gradient echo (SPGR), fat saturated 3D T2^a GRE, and short inversion recovery (STIR) sequences.^{a,c} In some horses, repositioned images were obtained to be perpendicular to the distal most part of the deep digital flexor tendon (DDFT). Selection of sequences depended in part on the results of the previous clinical investigations. Both forefeet were examined routinely.

Nuclear scintigraphic images were assessed subjectively and objectively.⁴ Uptake of the radiopharmaceutical in the navicular bone in solar views was graded as a normal (the ratio of uptake in the navicular bone and the peripheral regions of the distal phalanx was <110%), mild (>110 and <120%), moderate (>120 and <140%), or marked (>140%) increase.⁴ MR images were analyzed and reported by one trained analyst (R.M.) and verified by the examining clinicians (S.D. and M.S.).

3. Results

The signalment, history, and clinical findings are summarized in Table 1. Thirteen horses had unilateral forelimb lameness and five were affected bilaterally. The horses ranged from 3 to 15 yr of age. The duration of lameness varied between 3 and 12 mo. All horses underwent radiographic examination, and 14 horses were examined using nuclear scintigraphy. The results are summarized in Table 2.

Seven horses (cases 1–7) had obvious lesions in the DDFT that were restricted to either the medial (2), lateral (4), or both lobes (1) and were considered to be the primary cause of lameness (Table 3). One horse (case 2) with bilateral lameness had bilateral lesions. Three horses had lesions restricted to the dorsal border of the tendon (cases 1, 5, and 6; Fig. 1), and three (cases 2–4) had core lesions (Fig. 2), one of which also had abnormalities of the dorsal border. Case 7 had a split in the lateral lobe of the DDFT, which extended to its insertion on the distal phalanx and also had an abnormal signal at the insertion of the medial lobe. The lesions varied in length (1.3–7.0 cm) but usually extended distally from the proximal border of the navicular bursa, although only in case 7 was the insertion involved. One horse (case 4) had a separate lesion in the pastern region that was detectable ultrasonographically. Lameness was eliminated by perineural analgesia of the palmar digital nerves in three horses (cases 1, 2, and 7) and was improved in another (case 5). In the remainder, perineural analgesia of the palmar nerves abolished the lameness. Intra-articular analgesia of the DIP joint was performed in six of these horses (cases 2–7) and resulted in substantial improvement in five. Analgesia of the navicular bursa was performed in four horses (cases 3 and 5–7) and produced significant improvement in lameness in three. No significant radiological abnormality was identified in any of these horses. Ultrasonographic examination failed to identify any of the lesions within the hoof. Nuclear scintigraphic examination was performed in five horses (cases 2, 3, and 5–7), and in two (cases 3 and 5), there was increased radiopharmaceutical uptake (IRU) in the lateral pool phase image of the lame limb in the region of the DDFT. In case 7, there was a marked focal IRU in the solar bone phase view in the region of insertion

Table 1. Age, Occupation, Lame Limb(s), Lameness Grade, and Response to Local Anesthetic Techniques

| Case No. | Age (yr) | Occupation | Lame Limb(s) | Lameness Grade (lamer limb)* | Response to Local Anesthesia of Lamer Limb | | | |
|----------|----------|------------|--------------|------------------------------|--|--------|---------|---------|
| | | | | | PD | P (AS) | DIP | NB |
| 1 | 14 | GP | RF | 2-4 | S | NP | NP | NP |
| 2 | 10 | SJ | LF>RF | 1-2 | S | NP | NC | NP |
| 3 | 7 | GP | RF | 2-4 | NC | S | I (80%) | I (80%) |
| 4 | 9 | GP | RF | 4-6 | NC | S | I (70%) | NP |
| 5 | 10 | E | LF | 4 | I (40%) | S | I (80%) | I (95%) |
| 6 | 8 | SJ | RF | 1-4 | NC | S | I (90%) | NC |
| 7 | 6 | SJ | LF | 2 | I (80%) | S | S | S |
| 8 | 10 | E | LF | 2-4 | I (60%) | S | NC | S |
| 9 | 3 | R | RF | 1-4 | S | NP | I (75%) | NP |
| 10 | 13 | SJ | RF>LF | 2-4 | I (20%) | S | NC | S |
| 11 | 7 | SJ | RF | 2-6 | I (40%) | S | I (90%) | S |
| 12 | 8 | E | RF | 4 | I (50%) | S | NC | NP |
| 13 | 6 | SJ | LF>RF | 2-4 | S | NP | I (60%) | S |
| 14 | 10 | E | LF | 2-4 | I (60%) | S | S | NP |
| 15 | 9 | GP | RF | 4 | S | NP | S | NP |
| 16 | 15 | SJ | LF>RF | 1-4 | I (20%) | S | I (80%) | NP |
| 17 | 9 | E | RF>LF | 4 | I (90%) | S | I (90%) | NC |
| 18 | 9 | E | RF | 2-4 | I (85%) | S | I (85%) | NP |

GP, general purpose; SJ, show jumping; E, eventing; R, racing; PD, palmar digital; P (AS), palmar (abaxial sesamoid); DIP, distal interphalangeal joint; NB, navicular bursa; NP, not performed; NC, no change; I, improved; S, sound (or lame on contralateral limb).

*The range reflects either variability within or between examination periods or assessment under different circumstances, e.g., straight lines and circles.

of the DDFT. Four horses (cases 2, 3, 5, and 6) also had a mild or moderate IRU in the navicular bone of the lame limb, three of which had abnormalities of the navicular bone detected using fat-suppressed MR images. Two additional horses (cases 11 and 13), with primary navicular bone lesions, also had sagittal splits in the DDFT (Fig. 3). These were bilateral in case 11, despite unilateral lameness.

Six horses (cases 8-13) had an abnormally bright signal in the navicular bone in fat-suppressed images as the primary abnormality (Table 3 and Figs. 4 and 5). One additional horse (case 14) had an abnormally low signal through the center of the navicular bone in the T1 and T2 weighted images (Fig. 6) and a more widespread bright signal in fat-suppressed images. Three horses (cases 8, 9, and 14) also had marked distension of the navicular bursa. In all seven horses, lameness was improved or eliminated by perineural analgesia of the palmar digital nerves. Intra-articular analgesia of the DIP joint improved the lameness in only four of the horses (cases 9, 11, 13, and 14) in which it was performed. Intra-theal analgesia of the navicular bursa removed the lameness in four horses (cases 8, 9, 11, and 13), including two with distension of the navicular bursa (cases 8 and 9). Radiolucent zones along the distal border of the navicular bone were the only radiological observation. Nuclear scintigraphy was performed in six horses (cases 8 and 10-14) and revealed focal IRU palmar to the navicular bone in the lateral pool images in two horses (cases 8 and 10). In the bone phase images, uptake

of radiopharmaceutical was normal or reduced in two horses (cases 8 and 12). In one horse (case 11), there was marked IRU in the navicular bone in the non-lame limb and moderate IRU in the lame limb. One horse (case 10) had marked and moderate IRU in the navicular bone of the lamer and less lame limbs respectively. Case 13, with bilateral lameness, had moderate IRU in both navicular bones. Case 14, with an abnormally low signal in the center of the navicular bone, had a corresponding intense, focal, marked IRU. Three additional horses (cases 6, 17, and 18), with other concurrent abnormalities detected using MRI, also had a bright signal within the navicular bone of the lame limb, but this was more localized than in cases 8-14. Two of these horses had moderate IRU in the navicular bone of the lame(r) limb (cases 17 and 18).

Two horses (cases 15 and 16) had primary abnormalities in the DIP joint, with evidence of osteoarthritis (Table 3). One horse also had mineralization within the distal sesamoidean impar ligament (DSIL). Lameness was improved by perineural analgesia of the palmar digital nerves in case 16 and was eliminated in case 15. Intra-articular analgesia of the DIP joint produced substantial improvement in both horses. Intra-theal analgesia of the navicular bursa had no effect in case 16. One horse (case 16) had radiographic evidence of mild modeling of the articular margins of the DIP joint. Nuclear scintigraphy revealed moderate IRU in the navicular bone of the less lame limb and mild IRU in the

RADIOLOGY

Table 2. Results of Radiographic and Nuclear Scintigraphic Examinations

| Case No. | Radiography | Nuclear Scintigraphy | |
|----------|---|---|--|
| | | Pool Phase | Bone Phase |
| 1 | Sole thin; horizontal solar border of distal phalanx | NP | NP |
| 2 | Several large lucent zones distal border NB | NAD | LF NB = 103% RF NB = 116% |
| 3 | NAD | RIU in region of DDFT (lateral view) | LF NB = 114% RF NB = 126% |
| 4 | NAD | NP | NP |
| 5 | Subtle decrease in corticomedullary demarcation in NB | RIU in region of DDFT (lateral view) | LF NB = 125% |
| 6 | NAD | NAD | LF NB = 121% RF NB = 100% |
| 7 | NAD | NAD | LF NB = 113% RF NB = 113% |
| 8 | NAD | RIU palmar to NB (lateral view) | Focal RIU lateral palmar process |
| 9 | NAD | NP | NP |
| 10 | 4 large lucent zones distal border NB; mild modelling articular margins DIP joint | RIU palmar to NB (lateral view) | LF NB = 125% RF NB = 143% |
| 11 | 7 large lucent zones distal border NB | RIU region of DDFT (lateral view) | LF NB = 150% RF NB = 137% |
| 12 | NAD | NAD | LF NB = 98% RF NB = 91% |
| 13 | NAD | NAD | LF NB = 113%; focal area 132% RF NB = 113%; focal area 129% |
| 14 | NAD | NAD | LF NB = 123%; focal area 197% RF NB = 119% |
| 15 | NAD | NP | NP |
| 16 | Modelling of articular margin of DIP joint | NAD | LF NB = 111% RF NB = 126% |
| 17 | NAD | RIU region of insertion of DDFT and DSIL (lateral view) | LF NB = 102% RF NB = 122% |
| 18 | Many lucent zones distal and lateral sloping border NB | RIU region of insertion of DDFT and DSIL (lateral view) | LF NB = 100% RF NB = 121% RIU insertion of DDFT and DSIL |

NAD, no abnormality detected; NB, navicular bone; NB, navicular bone; % refers to the ratio of the mean counts per cell in the NB compared with the mean value for the peripheral regions of the distal phalanx measured in solar views (Dyson 2001); NP, not performed; NAD, no abnormality detected; RIU, region of increased uptake of radiopharmaceutical.

lamer limb in case 16, but no abnormality associated with the DIP joint.

Two horses (cases 17 and 18) had several abnormalities in the region of the DSIL and insertion of the DDFT, the navicular bone, and the DIP joint (Table 3). Lameness was substantially improved by perineural analgesia of the palmar digital nerves and abolished by palmar nerve blocks. Intra-articular analgesia of the DIP joint resulted in marked improvement in lameness, but intra-the-

cal analgesia of the navicular bursa, performed only in case 18, did not alter the lameness. Radiographic examination revealed many lucent zones along the distal and lateral sloping borders of the navicular bone in case 18. Nuclear scintigraphic examination revealed increased IRU in lateral pool phase images of the lamer limb in the region of insertion of the DDFT and DSIL and moderate IRU in the navicular bone in bone phase images of both horses.

Table 3. Results of Magnetic Resonance Imaging†

| Case No. | Observations |
|----------|---|
| 1 | Thin sole and collapsed heels LF and RF. Mineralization within the cartilage of the medial aspect of the DIP joint, with no evidence of cartilage or subchondral bone roughening. Enlargement of medial branch of DDFT, and loss of gap between it and navicular bone; rough dorsal border of DDFT, with a flap displaced dorsally. |
| 2 | LF. Linear bright signal in DDFT from proximal limit of navicular bursa to proximal aspect of NB in lateral branch. Dorsal aspect of DDFT roughened. Mild distension DFTS. Distension DIP joint capsule. RF. Bright signal in DDFT and rough dorsal border as LF. Mild distension DFTS. |
| 3 | Core lesion in medial branch of DDFT from level of proximal aspect of navicular bursa to distal aspect of NB. Tissue protruding into navicular bursa. Distension of navicular bursa and evidence of chronic inflammation. Roughened medial flexor surface of NB. |
| 4 | 2 core lesions in lateral branch of DDF in pastern region; separate core lesions extending from proximal level of navicular bursa to distal aspect of NB. Distension DFTS. |
| 5 | Bright signal in NB in fat saturated images. Lesion in dorsal border of lateral branch of DDFT proximal to NB. |
| 6 | Lesion in dorsal border of lateral branch of DDFT, extending from proximal aspect of navicular bursa to distal aspect of NB, with dorsopalmar split at level of NB. Bright signal on dorsal aspect of distal phalanx LF and RF. |
| 7 | Sagittal split in lateral branch of DDFT extending from distal aspect of proximal phalanx to insertion; abnormal signal in medial branch at insertion. Bright signal in NB in fat suppressed images. Bright signal in distal phalanx at DDFT insertion in fat suppressed images. |
| 8 | Distension of navicular bursa, with fibrous strands crossing it. Irregular outline of dorsal aspect of DDFT at proximal pouch of navicular bursa. Bright signal in NB in fat saturated images. Mineralization in DSIL adjacent to midline. |
| 9 | Bright signal in NB in central portion. Unusual vasculature medial aspect of NB. Linear increased signal distal border NB laterally. |
| 10 | RF. Enlarged navicular bursa with synovial proliferation. Distension and synovial proliferation DIP joint capsule. Osteophyte proximal aspect distal phalanx. Large synovial invaginations distal border NB. Areas of bright signal in NB in fat saturated images. Increased vasculature in NB. LF. As above. |
| 11 | RF. Rough flexor border of NB. Marked loss of fat content in medulla of NB. Bright signal throughout the NB in fat suppressed images. Split in lateral branch of DDFT at level of navicular bursa. LF. Split in DDFT at level of navicular bursa. |
| 12 | Bright signal in NB bilaterally particularly in midline, in fat suppressed images. Mineralization in DSIL biaxially and bilaterally. |
| 13 | Bright signal in NB bilaterally in fat suppressed images, especially towards midline. Distension of DIP joint capsule and navicular bursa. LF. Rough dorsal border of DDFT at level of navicular bursa. |
| 14 | Very low or absent signal in the middle of the navicular bone, extending from proximal to distal borders, compatible with mineralization; bright signal in large part of NB in fat suppressed images. Distension of the navicular bursa and synovial proliferation. Roughened dorsal border of DDFT. |
| 15 | Rough articular margin of subchondral bone of distal phalanx and defect in subchondral bone margin distal aspect of middle phalanx. Loss of signal in articular cartilage. Mineralization in DSIL medial to midline. |
| 16 | Loss of signal in articular cartilage in DIP joint; irregular outline of cartilage; subchondral bone of distal phalanx irregularly thickened. Synovial proliferation dorsal and palmar pouches DIP joint. Irregular proximal and distal borders of NB. Distension PIP joint capsule RF only. |
| 17 | Abnormal signal in cartilage lateral aspect of distal phalanx. Bright signal in lateral aspect of NB. Mineralization in lateral aspect of DSIL, with abnormal fibre pattern in DSIL. Increased fluid in DIP joint and navicular bursa. |
| 18 | Areas of fluid accumulation and irregular signal associated with most distal aspect of DDFT and its insertion. Distal border fragments in DSIL on medial and lateral aspects of NB, with associated areas of bright signal in adjacent NB and in body of bone. Similar distal border fragments in LF, but normal NB. |

†No abnormalities were detected in the non-lame limb, unless stated.

NB, navicular bone; DFTS, digital flexor tendon sheath; PIP, proximal interphalangeal joint.

4. Discussion

MRI is not a screening tool, and it is essential to be focused, based on the results of a previous comprehensive clinical investigation, so that examination is limited to a specific region and appropriate imaging sequences are selected based on the suspected le-

sion. Interpretation of the findings in this study was based on comparison with previous cadaver studies of normal horses^d and published normal studies,^{14,17} and also with horses with pathological abnormalities of the foot verified at post-mortem^d or previously recorded.^{11-13,18}

RADIOLOGY



Fig. 1. Sagittal 3D T2^a GRE image of the left front foot of case 2. There is a linear bright signal involving the dorsal border of the DDFT extending proximal to the navicular bone (arrow).

In this series of 18 horses, abnormalities of the DIP joint cartilage and subchondral bone, lesions of the DDFT, abnormalities of the navicular bursa, pathological changes in the navicular bone, and abnormal signal in the DSIL were identified. There was an interesting correlation with previously performed diagnostic techniques. Of the seven horses with primary DDFT lesions, five of six responded to analgesia of the DIP joint and three of four to analgesia of the navicular bursa. Four of six horses with primary navicular bone lesions responded to analgesia of the DIP joint, and all horses in which analgesia of the navicular bursa was performed had a positive response. This study verified the potential sensitivity and usefulness of high-quality pool and bone phase scintigraphic images in localizing the anatomical position of lesions in many horses. Superimposition of radiographic and scintigraphic images was sometimes required for accurate anatomical localization of IRU. Quantitative image analysis⁴ helped to determine the potential significance of IRU in the navicular bone. However, radiopharmaceutical uptake was normal or reduced in two horses with primary abnormalities of the navicular bone seen using MRI. Moderate or marked IRU was identified in the navicular bone of non-lame limbs of two of the nine unilaterally lame horses in which scintigraphy was performed.

The majority⁷ of DDFT lesions were located proximal to the navicular bone, a region inaccessible for ultrasonographic evaluation through the sole, and an area where the ultrasound beam cannot be perpendicular to the line of the fibers if imaging

through the heel, although changes in size can be identified. Dystrophic mineralization may also be seen, but was not present in any of these horses. The lesions were usually restricted to either the medial or lateral lobe of the tendon, thus those lesions ex-

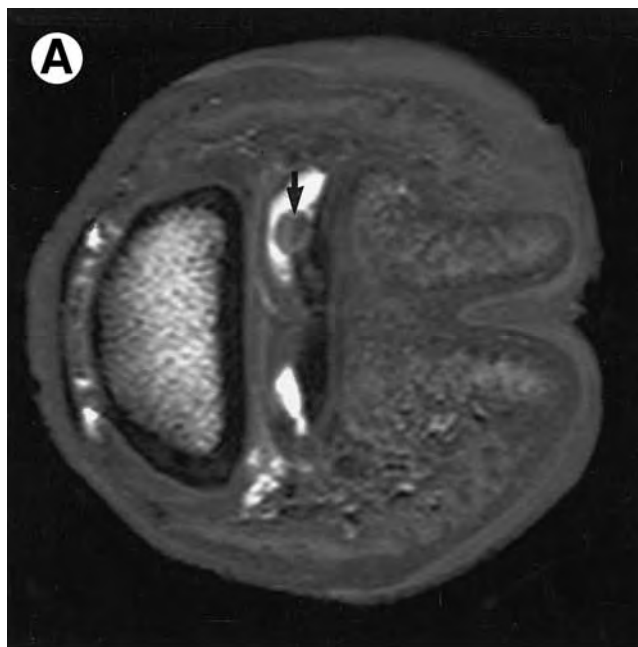


Fig. 2. (a) Transverse 3D T2^a GRE image of the right front foot of case 3. Medial is proximal, and dorsal is to the left. The medial lobe of the DDFT is enlarged and has a central region of bright signal. There is tissue protruding from the dorsal border of the DDFT (arrow) into the navicular bursa, which is distended. (b) Sagittal 3D spoiled gradient echo image of the right front foot of case 3. There is an abnormal bright signal in the center of the enlarged DDFT, proximal to the navicular bone (arrow).

RADIOLOGY

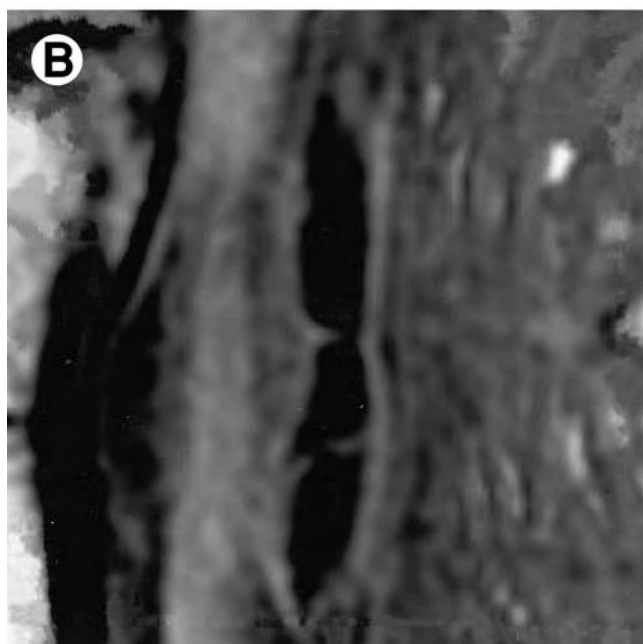
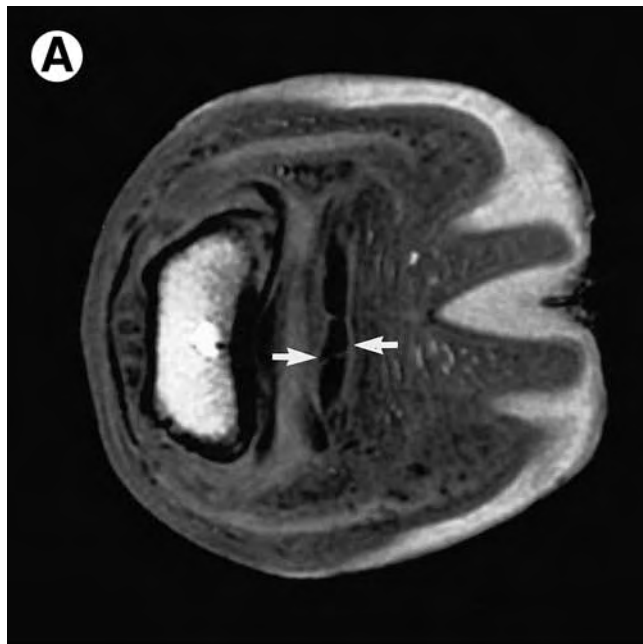


Fig. 3. (a) Transverse spoiled GRE image of the right front foot of case 11. Lateral is distal and dorsal is to the left. There is a sagittal full-thickness split in the lateral lobe of the DDFT (arrow). (b) The same lesion as in Figure 3a, magnified. This full-thickness split was confirmed at post-mortem.

tending to the level of the navicular bone were not identified by ultrasonographic imaging through the frog. The site of these lesions correlated with the location of IRU in a lateral pool phase scintigraphic image in two of four horses. Lesions extended to the insertion of the DDFT on the distal phalanx in only one horse, and only in this horse was IRU identified in this region in bone phase scintigraphic

images. However two horses with MRI abnormalities in the region of insertion of the DDFT and DSIL did have IRU in this region in lateral pool phase images. Lesions of the DDFT within the hoof capsule have previously been identified post-mortem¹ by bursoscopy of the navicular bursa^{19,e} and us-

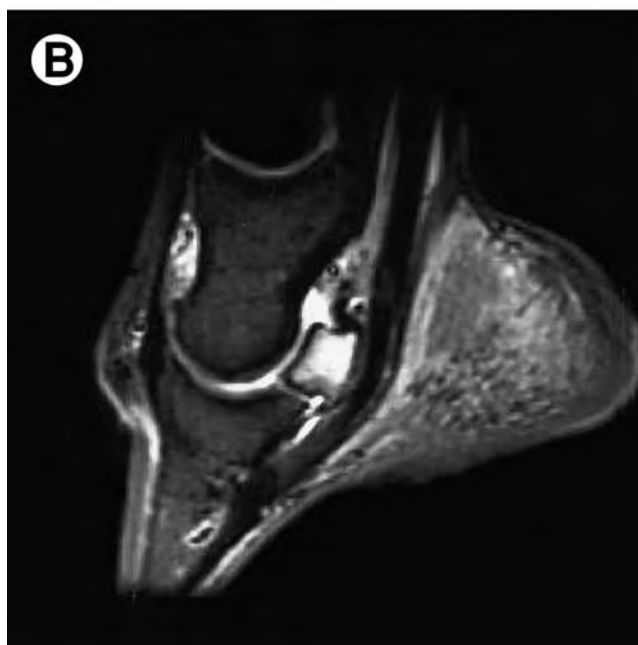
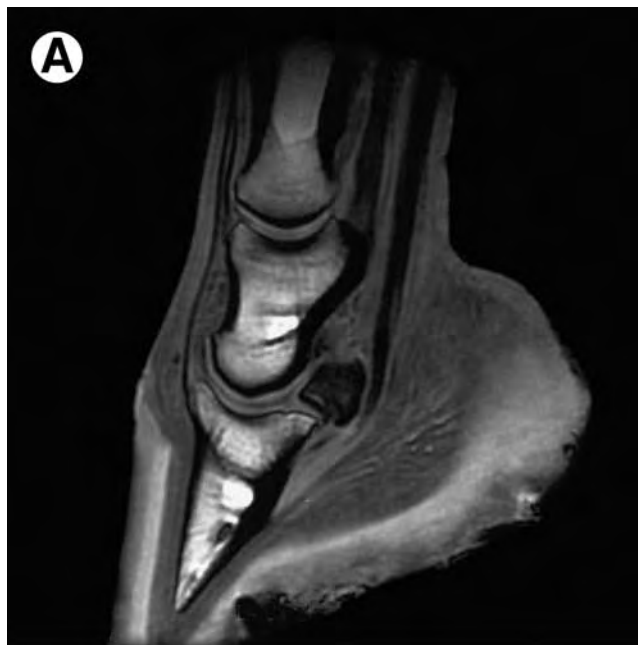


Fig. 4. (a) Sagittal T1 weighted image of the right front foot of case 11. There is marked loss of fat signal within the navicular bone. Compare with Figure 4b. (b) Sagittal fat-suppressed image of the right front foot of case 11. There is an extremely bright signal throughout the navicular bone compatible with bone edema or necrosis. Compare with the proximal and middle phalanges and with Figure 4a.

RADIOLOGY



Fig. 5. Dorsal fat-suppressed T2 weighted image of the right front foot of case 12. Note the bright signal in the central one-third of the navicular bone.

ing CT,^f but based on this study and that of Nowak's,^f it is likely that the incidence has previously been underestimated. Fifteen of 78 horses examined using CT had lesions in the DDFT in the digit, without associated abnormalities of the navicular bone; the most common site was proximal to the navicular bone,^f as in this study.

Two horses had MRI evidence of osteoarthritis of the DIP joint, one of which had mild periarticular osteophyte formation detected radiographically. Radiography was an insensitive indicator of pathological abnormalities of the subchondral bone and articular cartilage, which were clearly demonstrated using MRI. There was normal radiopharmaceutical uptake in the region of the DIP joint in both of these horses. Distension of the DIP joint capsule was seen frequently and not restricted to the lame limb, but enlargement of the navicular bursa was only seen in the lame limb(s) and was identified in eight horses (cases 4, 7, 8, 11, 13–15, and 17). Three of these horses had IRU palmar to the navicular bone in lateral pool phase images. Distension of the navicular bursa can be identified ultrasonographically through the frog, or the heel bulbs, but only a limited portion can be examined properly. Previously the only method of verification of navicular bursitis was by invasive bursoscopy, which is a useful diagnostic method and has been used to identify DDFT and DSIL lesions and erosions of the flexor surface of navicular bone.^{19,e} However examination is limited to the proximal pouch of the bursa and the immediately adjacent structures. Although changes in outline of the navicular bone

were detected in standard sequences, and a centrally located very low signal was seen in one horse, fat-suppressed images were required to identify other changes in internal architecture of the navicular bone, which were identified in a further 11

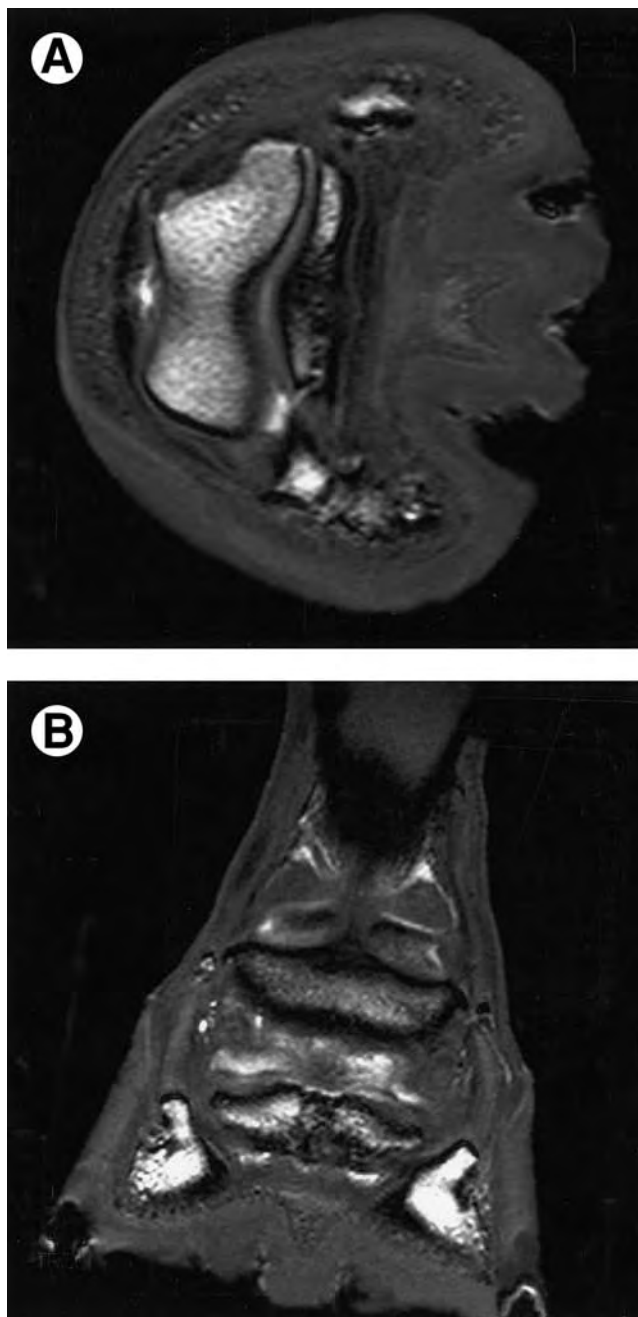


Fig. 6. (a) Transverse 3D T2^a GRE image of the left front foot of case 14. There is low signal in the center of the navicular bone extending from the dorsal cortex to the flexor cortex. This is consistent with mineralization within the navicular bone. (b) Dorsal 3D T2^a GRE image of the left front foot of case 14. There is low signal extending from the proximal to distal cortices in the center of the bone, consistent with mineralization within the bone.

horses. Eleven of these 12 horses were examined scintigraphically, and marked or moderate IRU was identified in the navicular bone in seven. An additional horse with a primary DDFT lesion also had roughening of the medial aspect of the flexor surface of the navicular bone associated with moderate IRU in the navicular bone. The bright signal in the navicular bone is compatible with bone edema or necrosis. The low signal in the central part of the navicular bone of case 14 is compatible with increased mineralization, possibly the result of a fracture.

Areas of low signal in the DSIL compatible with mineralized fragments were identified by MRI in five horses (cases 8, 12, 15, 17, and 18), the clinical significance of which remains unclear. In two horses (cases 12 and 18), there were medial and lateral fragments bilaterally. None of the fragments was identified radiographically in any horse. Four of these horses also had bright signal in the navicular bone. The incidence of fragments in the DSIL was higher in a post-mortem study of horses with navicular disease compared with age-matched controls.²⁰

This study clearly highlights the limitations of radiographic examination in some horses with palmar foot pain. It does however demonstrate the potential value of intra-articular analgesia of the DIP joint and intra-theal analgesia of the navicular bursa in helping to localize pain. Nuclear scintigraphic examination was helpful but potentially misleading in some horses. The relationship between lesions identified using MRI and pain causing lameness is at this stage speculative, but in the majority of horses, major lesions were confined to the lame limb in unilaterally lame horses and were bilateral in those with bilateral lameness. Lesions of the DDFT and the navicular bone were seen either alone or in combination, and the relationship between these lesions and what has previously been referred to as navicular disease remains open to question.

The interpretation of the MRI findings in this study must be viewed in light of the other diagnostic information available because only one of the horses was examined post-mortem. It is hoped that as a result of more accurate identification of the causes of foot pain, more appropriate treatment regimens can be developed, and in the future more accurate prognostic information will be available.

We thank Dr. Russ Tucker for invaluable assistance in the preliminary development of imaging sequences, the Animal Health Trust anesthetists and yard staff, and the referring veterinary surgeons. We also thank John Wilkinson for production of the figures.

References and Footnotes

1. Dyson S, Kidd L. A comparison of responses to analgesia of the navicular bursa and intra-articular analgesia of the distal

- interphalangeal joint in 59 horses. *Equine Vet J* 1993;25:93–98.
2. Schumacher J, Schumacher J, deGraves F, et al. A comparison of two volumes of local analgesic solution in the distal interphalangeal joint of horses with lameness caused by solar toe or heel pain. *Equine Vet J* 2001;33:265–268.
3. Schumacher J, Schumacher J, deGraves F, et al. A comparison of the effects of local analgesic solution in the navicular bursa of horses with lameness caused by solar toe or heel pain. *Equine Vet J* 2001;33:386–389.
4. Dyson S. Subjective and quantitative scintigraphic assessment of the equine foot and its relationship with foot pain. *Equine Vet J* 2002;34:164–170.
5. Sage A, Turner A. Ultrasonography in the horses with palmar foot pain: 13 cases, in *Proceedings*. Am Assoc Equine Pract 2000;380–381.
6. Busoni V, Denoix J-M. Ultrasonography of the podotrochlear apparatus in the horse using a transcuneal approach: technique and reference images. *Vet Radiol Ultrasound* 2001;42:534–540.
7. Tietje S. Computed tomography of the navicular bone region in the horse: a comparison with radiographic documentation. *Pferdheilkunde* 1995;11:51–62.
8. Ruohoniemi M, Tevahartiala P. Computed tomographic evaluation of finnhorse cadaver feet with radiographically problematic findings on the flexor surface of the navicular bone. *Vet Radiol Ultrasound* 1999;40:225–281.
9. Tietje S, Nowak M, Petzoldt S, et al. Computed tomographic evaluation of the distal aspect of the deep digital flexor tendon (DDFT) in horses. *Pferdheilkunde* 2001;17:21–29.
10. Tucker R, Sande R. Computed tomography and magnetic resonance imaging in equine musculoskeletal conditions. *Vet Clin North Am [Equine Pract]* 2001;17:145–157.
11. Denoix J-M, Crevier N, Roger B, et al. Magnetic resonance imaging of the equine foot. *Vet Radiol Ultrasound* 1993;34:405–411.
12. Whitton C, Buckley C, Donovan T, et al. The diagnosis of lameness associated with distal limb pathology in a horse: a comparison of radiography, computed tomography and magnetic resonance imaging. *Equine Vet J* 1998;155:223–229.
13. Widmer A, Buckwater K, Fessler J, et al. Use of radiography, computed tomography and magnetic resonance imaging for evaluation of navicular syndrome in the horse. *Vet Radiol Ultrasound* 2000;41:108–116.
14. Kleiter M, Kneissl S, Stanek C, et al. Evaluation of magnetic resonance imaging techniques in the equine digit. *Vet Radiol Ultrasound* 1999;40:15–22.
15. Butler J, Colles C, Dyson S, et al. The foot, pastern and fetlock. In: *Clinical radiology of the horse*, 2nd ed. Oxford, England Blackwell Scientific 2000;27–130.
16. Dyson S, Lakhani K, Wood J. Factors influencing blood flow in the equine digit and their effect on uptake of ^{99m}technetium methylene diphosphonate into bone. *Equine Vet J* 2001;33:591–598.
17. Kotani H, Taura Y, Sakai A, et al. Antemortem evaluation of magnetic resonance imaging of the equine flexor tendon. *J Vet Med Sci* 2000;62:81–84.
18. Ruohoniemi M, Karkkainen M, Tervahartiala P. Evaluation of the variably ossified collateral cartilages of the distal phalanx and adjacent anatomical structures in the Finnhorse with computed tomography and magnetic resonance imaging. *Vet Radiol Ultrasound* 1997;38:344–351.
19. Dyson S. The puzzle of distal interphalangeal joint pain. *Equine Vet Edu* 1998;10:119–125.
20. Wright I, Kidd L, Thorp B. Gross, histological and histomorphometric features of the navicular bone and related structures in the horse. *Equine Vet J* 1998;30:220–234.

^aIt is beyond the scope of this paper to describe in depth the different imaging sequences that can be used to obtain MR images. Different image sequences are used to highlight different anatomical structures and to demonstrate different types of lesions. Selection of image sequence is also influenced by the time for image acquisition. In T2 weighted images, cortical bone has a

RADIOLOGY

low signal (appears black), whereas the medullary bone has a higher signal (looks brighter) because of increased fat content. Tendons and ligaments also have low signal (black). Synovial fluid has a high signal (appears white). Fat-suppressed images are used to suppress the bright signal of fat to be able to detect bright signal caused by bone edema or bone necrosis.

^bDyson S, Murray R, Schramme M, et al.

Magnetic resonance imaging of the equine foot: 15 horses. *Equine Vet J* Submitted 2002.

^cWhitton C, Murray R, Dyson S. Magnetic resonance imaging. In: Ross M, Dyson S, eds. *Diagnosis and management of lameness in the horse*. Philadelphia, PA: W.B. Saunders. Submitted 2002.

^dWhitton C, Schramme M, Dyson S. Unpublished data. 2001.

^eDyson S, Whitton C. Unpublished data. 1999.

^fNowak M. Personal communication. 2000.

^gIntra-Epicaine, Arnolds Veterinary Products Ltd., Cartmel Drive, Harlescott, Shrewsbury SY1 3TB, United Kingdom.